Supporting Information

A Guanidinium-based Mn^{4+}-doped Red-emitting Hybrid Phosphor with High Stability

Hong Ming, Yifei Zhao, Yayun Zhou*, Shuai Zhang, Yuanjing Wang, Enhai Song, Zhiguo Xia, and Qinyuan Zhang*

State Key Laboratory of Luminescent Materials and Devices, and Guangdong Provincial Key Laboratory of Fiber Laser Materials and Applied Techniques, South China University of Technology, Guangzhou 510641, China

**** Corresponding author E-mail**: zhou-yayun@foxmail.com, qyzhang@scut.edu.cn*

1. Figures

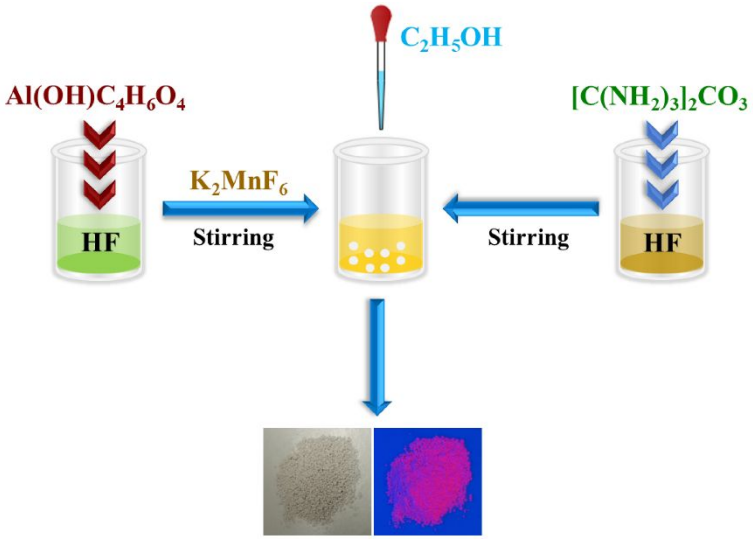

Figure S1. Schematic diagram for the synthesis of organic-inorganic hybrid red phosphor $GA_3AlF_6:Mn^{4+}$ and digital photographs of the obtained powders under (a) the natural light and (b) the blue light irradiation, respectively.

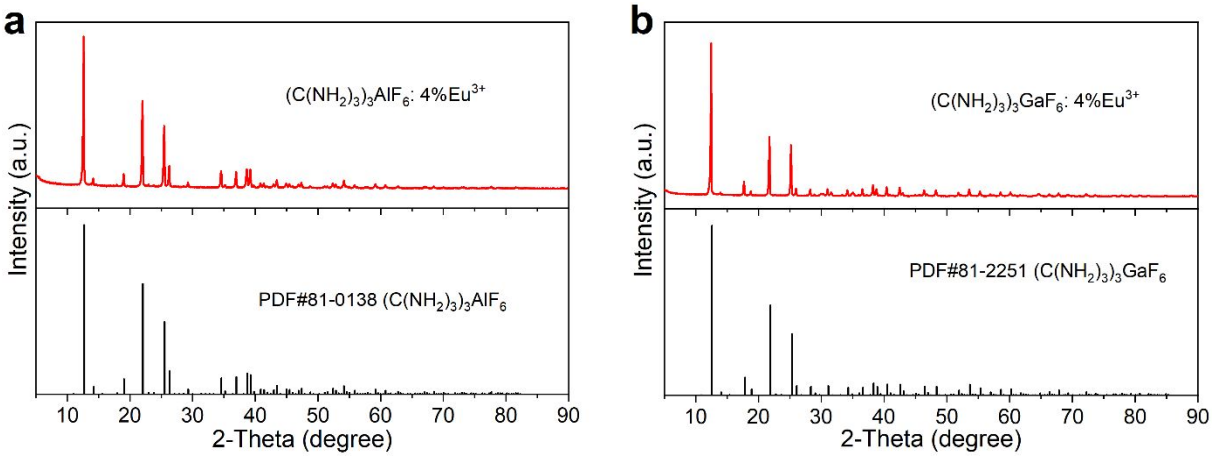

Figure S2. XRD patterns of Eu^{3+}-doped $[C(NH_2)_3]_3AlF_6:4\%Eu^{3+}$ (a) and $[C(NH_2)_3]_3GaF_6:4\%Eu^{3+}$ (b).

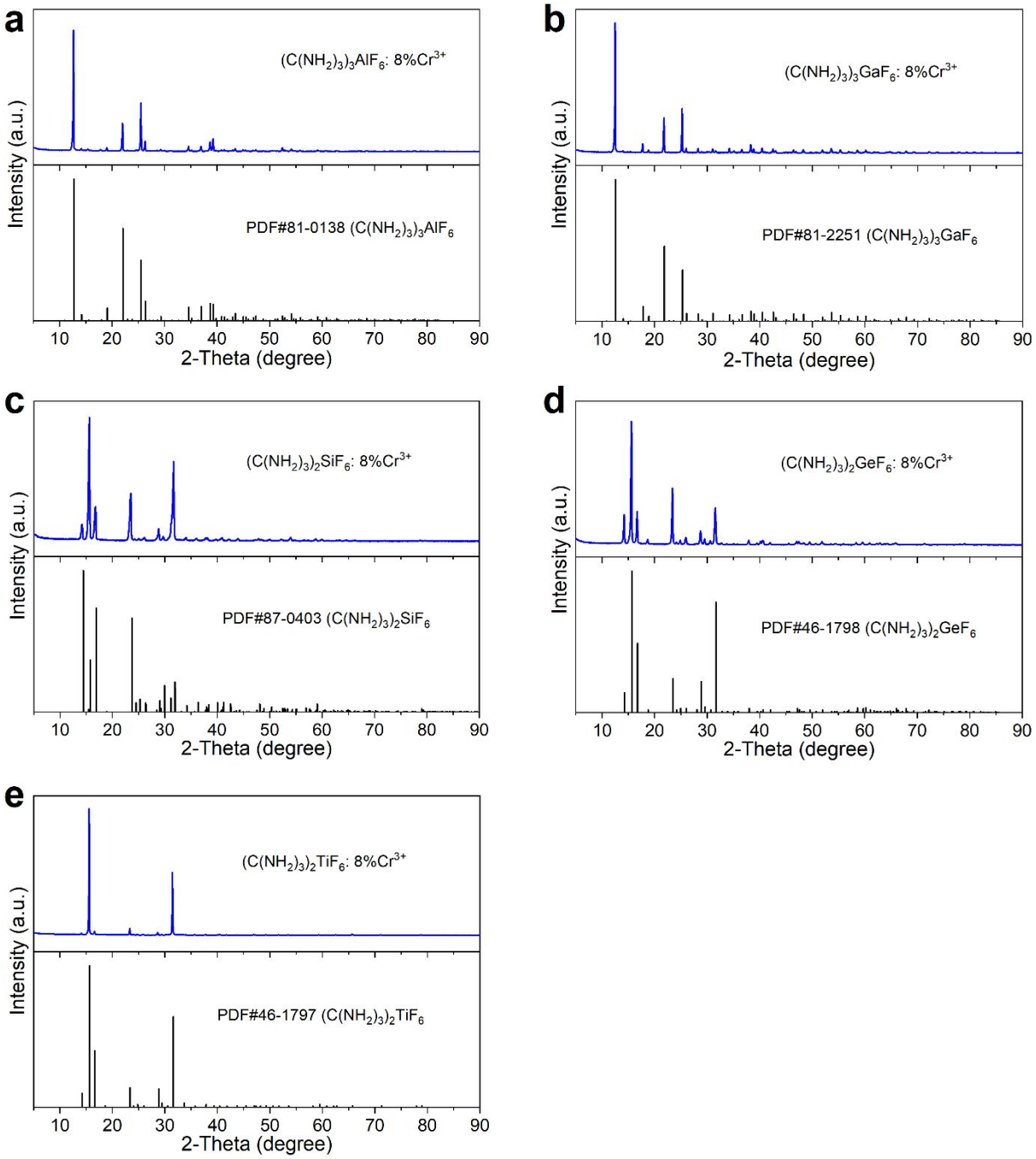

Figure S3. XRD patterns of Cr^{3+}-doped $[C(NH_2)_3]_3AlF_6$:8%Cr^{3+} (a), $[C(NH_2)_3]_3GaF_6$:8%Cr^{3+} (b), $[C(NH_2)_3]_2SiF_6$:8%Cr^{3+} (c), $[C(NH_2)_3]_2GeF_6$:8%Cr^{3+} (d), and $[C(NH_2)_3]_2TiF_6$:8%Cr^{3+} (e).

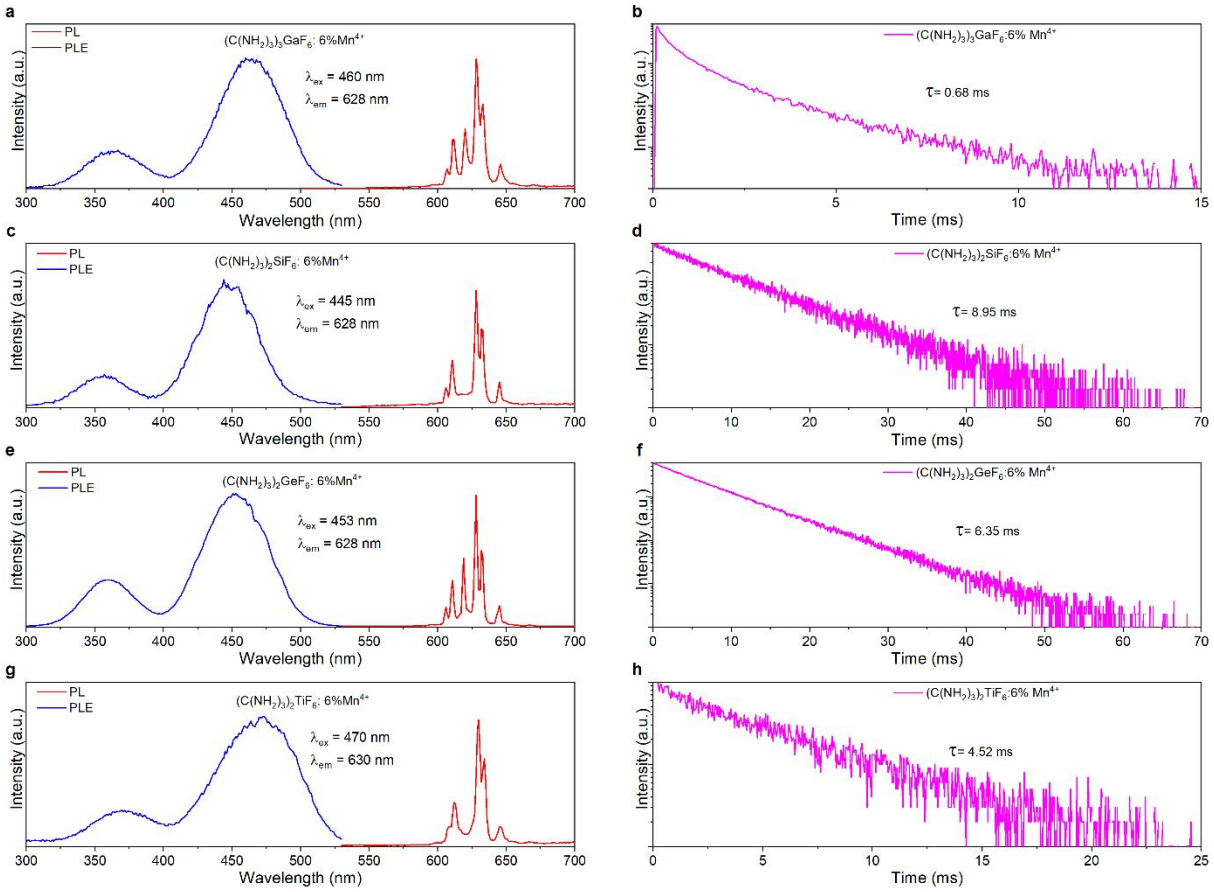

Figure S4. (a) PLE and PL spectra, and (b) PL decay curve of Mn^{4+}-doped $[C(NH_2)_3]_3GaF_6$:6%Mn^{4+}; (c) PLE and PL spectra, and (d) PL decay curve of Mn^{4+}-doped $[C(NH_2)_3]_2SiF_6$:6%Mn^{4+}; (e) PLE and PL spectra, and (f) PL decay curve of Mn^{4+}-doped $[C(NH_2)_3]_2GeF_6$:6%Mn^{4+}; (g) PLE and PL spectra, and (h) PL decay curve of Mn^{4+}-doped $[C(NH_2)_3]_2TiF_6$:6%Mn^{4+}.

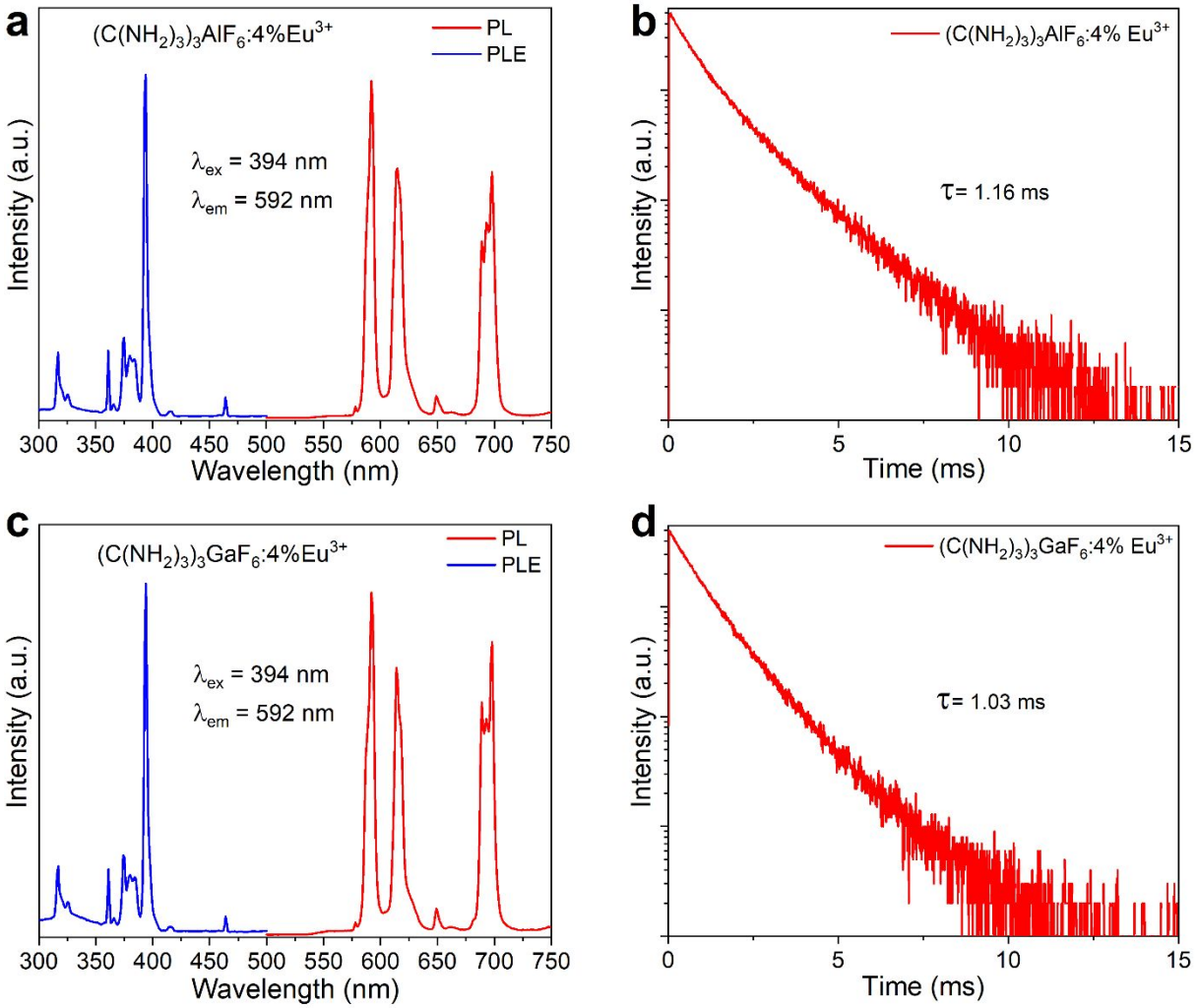

Figure S5. (a) PLE and PL spectra, and (b) PL decay curve of Eu^{3+}-doped $[C(NH_2)_3]_3AlF_6$:4%Eu^{3+}; (c) PLE and PL spectra, and (d) PL decay curve of Eu^{3+}-doped $[C(NH_2)_3]_3GaF_6$:4%Eu^{3+}.

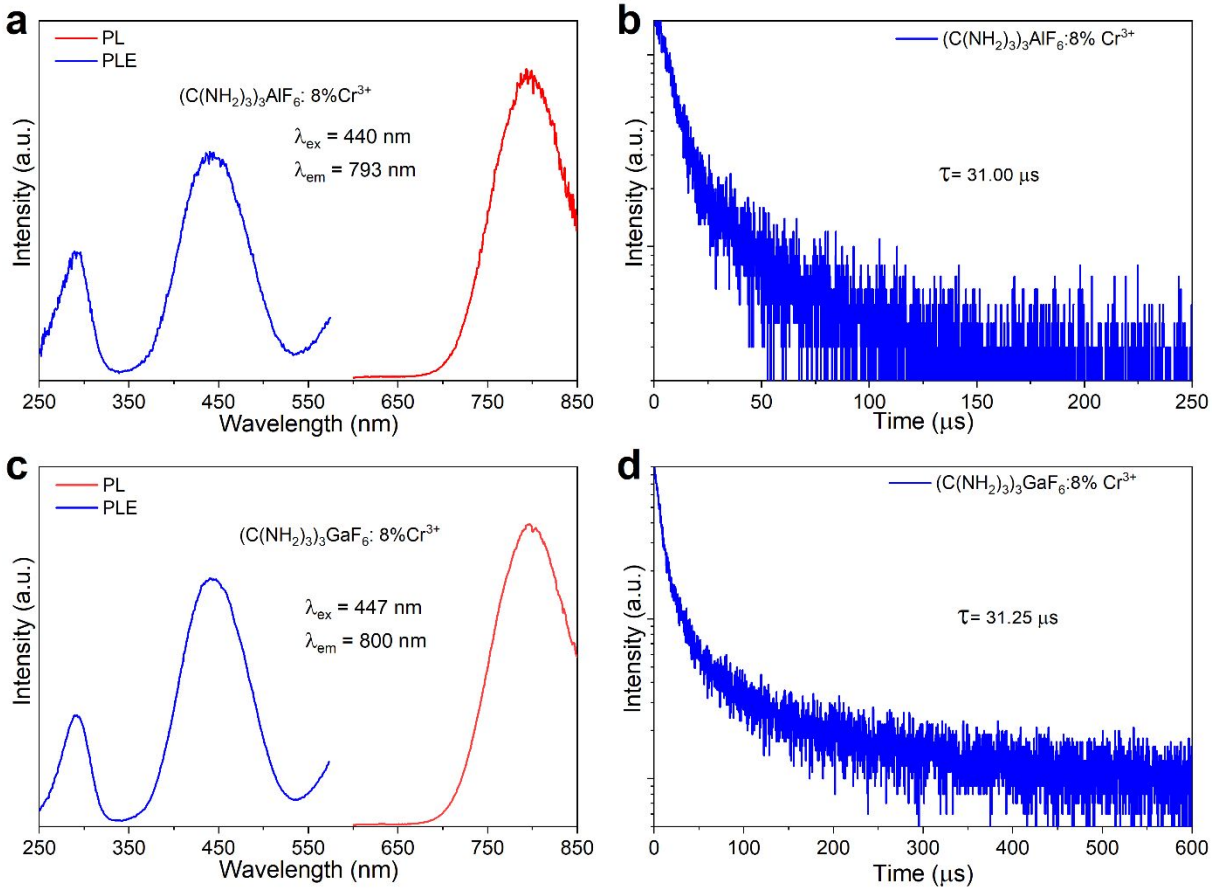

Figure S6. (a) PLE and PL spectra, and (b) PL decay curve of Cr^{3+}-doped $[C(NH_2)_3]_3AlF_6$:8%Cr^{3+}; (c) PLE and PL spectra, and (d) PL decay curve of Cr^{3+}-doped $[C(NH_2)_3]_3GaF_6$:8%Cr^{3+}.

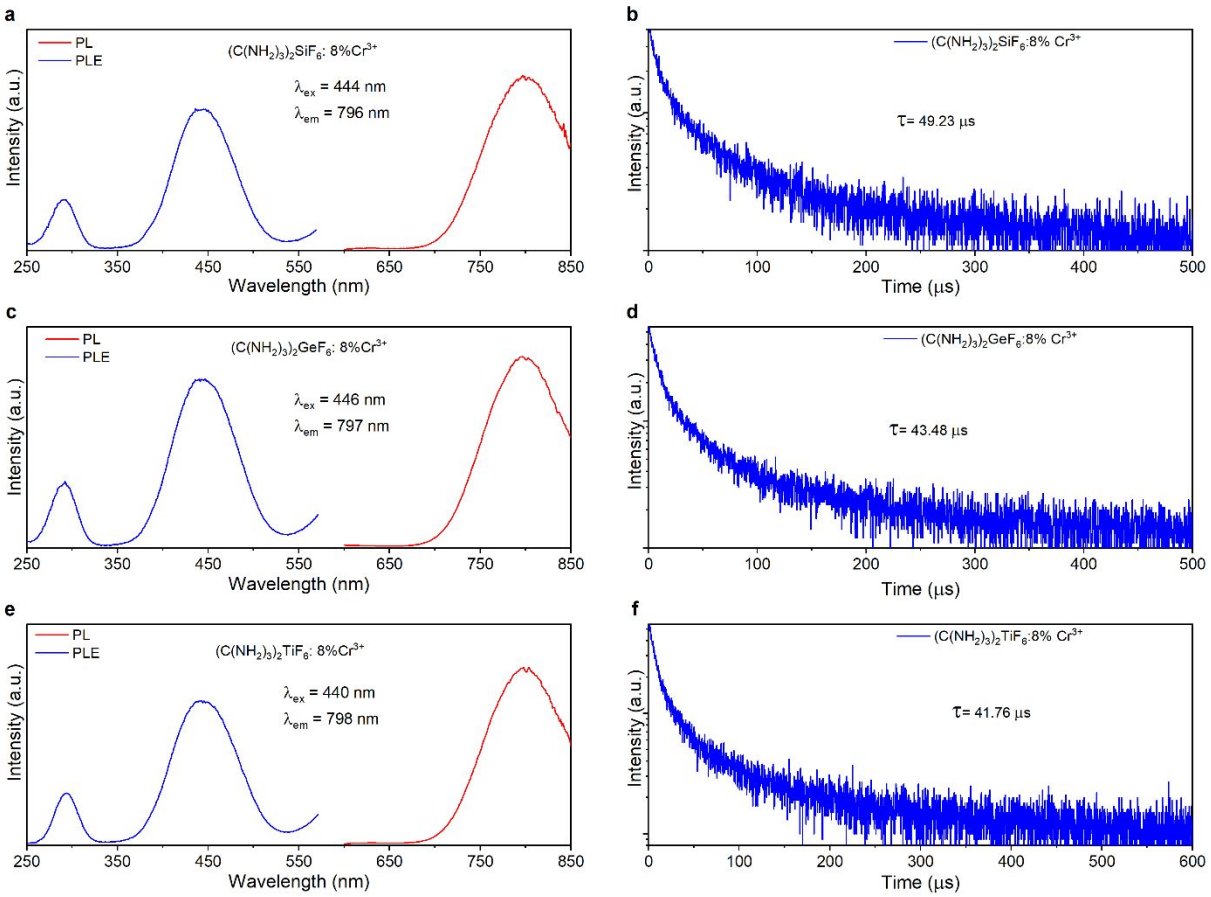

Figure S7. (a) PLE and PL spectra, and (b) PL decay curve of Cr^{3+}-doped $[C(NH_2)_3]_2SiF_6$:8%Cr^{3+}; (c) PLE and PL spectra, and (d) PL decay curve of Cr^{3+}-doped $[C(NH_2)_3]_2GeF_6$:8%Cr^{3+}; (e) PLE and PL spectra, and (f) PL decay curve of Cr^{3+}-doped $[C(NH_2)_3]_2TiF_6$:8%Cr^{3+}.

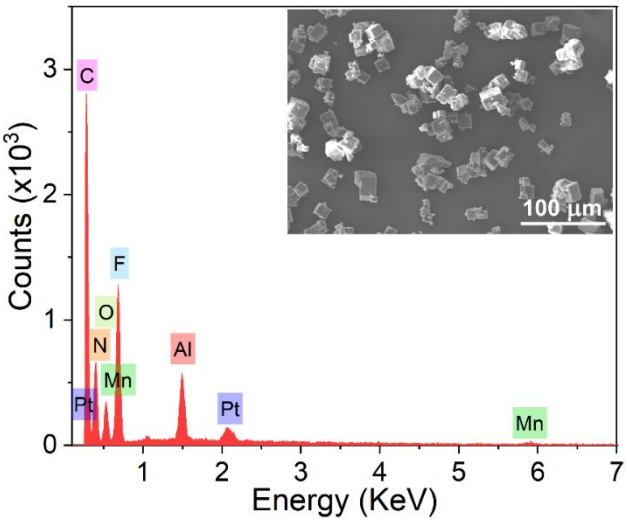

Figure S8. SEM image and the corresponding EDS spectrum of GA_3AlF_6:Mn^{4+}.

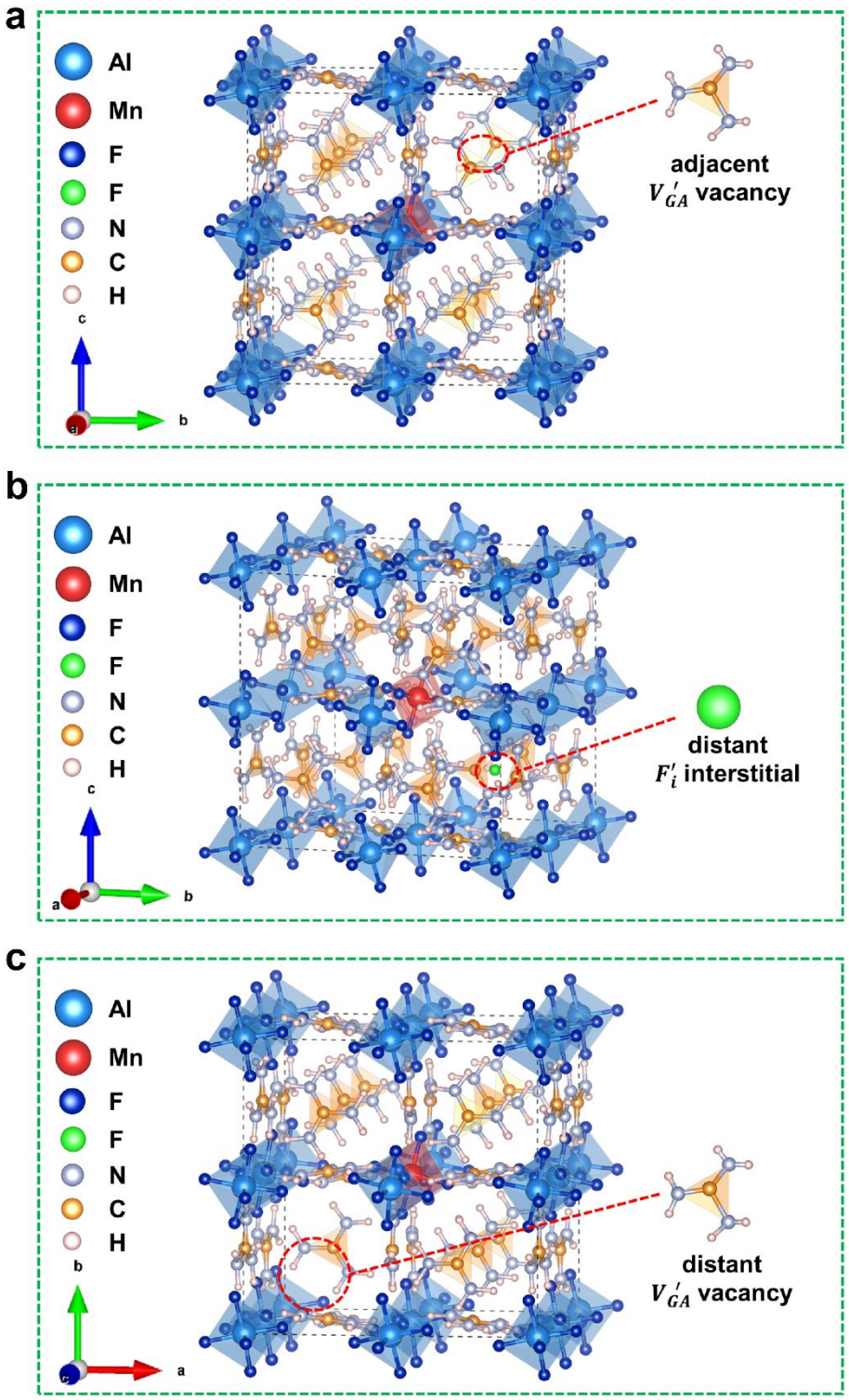

Figure S9. Three possible Mn^{4+}-doped structural models after structure optimization based on DFT: (a) Mn^{4+} substituting Al-site ($Mn_{Al}^{\cdot}$), and simultaneously producing an adjacent V'_{GA} defect; (b) Mn^{4+} substituting Al-site ($Mn_{Al}^{\cdot}$) while a distant F'_i defect was produced simultaneously; and (c) Mn^{4+} occupying Al-site ($Mn_{Al}^{\cdot}$) with the appearance of a distant V'_{GA} at the mean time.

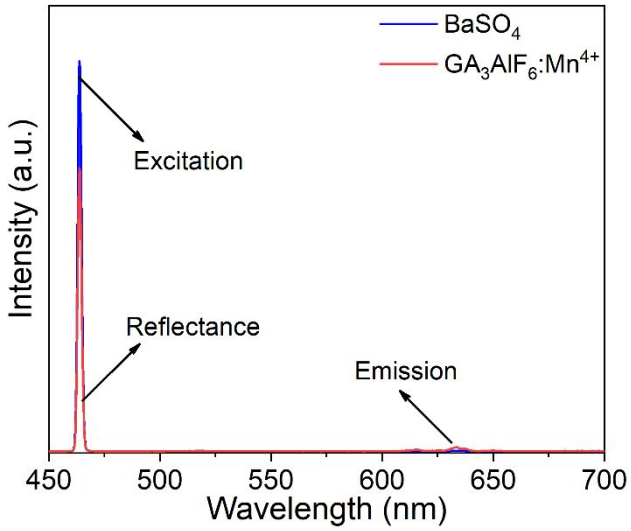

Figure S10. PL spectra of GA_3AlF_6:2.43%Mn^{4+} and reference sample measured using an integrating sphere for QE.

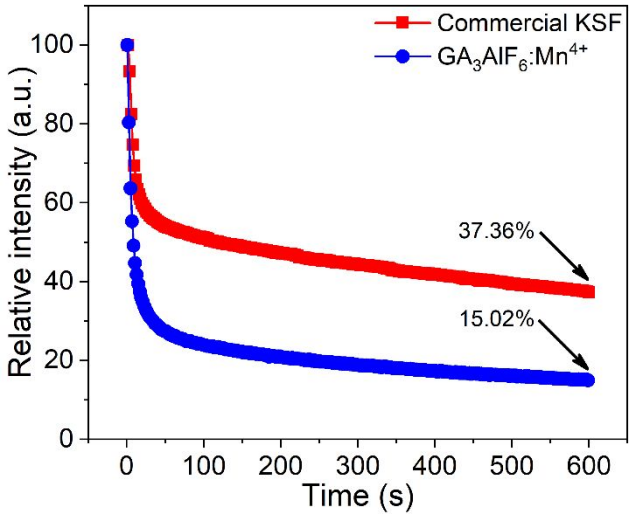

Figure S11. The relative PL intensity changes of commercial KSF phosphor and GA_3AlF_6:Mn^{4+} hybrid phosphor immersed in water for 10 min.

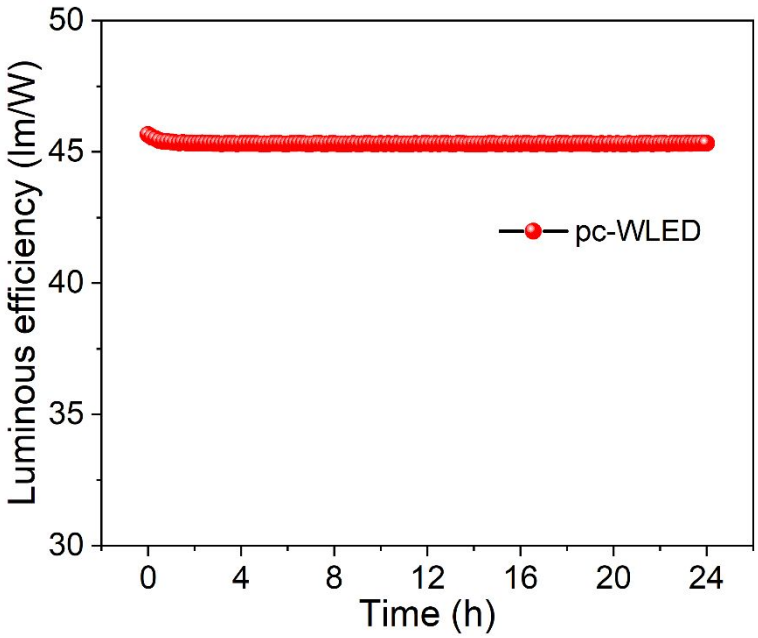

Figure S12. The luminous efficiency change curve of continuously lighting the pc-WLED device for 24 h.

2. Tables

Table S1. Schemes of different molar ratios of $Al(OH)C_4H_6O_4$ to K_2MnF_6 for the synthesis of organic-inorganic hybrid red phosphor $GA_3AlF_6:Mn^{4+}$ and the actual doping amount of Mn^{4+} suggested by the ICP-OES results.

samples	Al : Mn (Molar ratio)	actual doping amount of Mn^{4+} (mol%)
1	100 : 1	0.68
2	100 : 3	1.66
3	100 : 6	2.43
4	100 : 9	4.53
5	100 : 12	6.65
6	100 : 15	7.41

Table S2. Rietveld refinement parameters of X-ray diffraction profiles of GA_3AlF_6. The numbers in parentheses are the estimated standard deviations of the last significant figure.

Formula	GA_3AlF_6
T/K	298
symmetry	cubic
space group	Pa-3
a, b, c/Å	13.9723(8)
α, β, γ/degree	90
Volume/Å^3	2727.7912(7)
Z	8
2θ-interval/degree	5-90
Rwp	14.75
Rp	11.03
gof	2.88

Table S3. Structural parameters of GA_3AlF_6 obtained from the Rietveld refinement of X-ray diffraction at room temperature. The numbers in parentheses are the estimated standard deviations of the last significant figure.

Atom	Site	*x*	*y*	*z*	Occ.	B_{iso} (Å^2)
Al1	4b	0	0.5	0	1.0000(0)	0.3145(0)
Al2	4a	0	0.5	0.5	1.0000(0)	0.3145(0)
F1	24d	0.0300(1)	0.6245(9)	0.0233(3)	1.0000(0)	0.1818(0)
F2	24d	0.0184(2)	0.6247(7)	0.4758(5)	1.0000(0)	0.1818(0)
C	24d	0.7740(2)	0.7653(3)	0.5157(8)	1.0000(0)	1.9987(0)
N1	24d	0.8656(7)	0.7508(7)	0.5135(7)	1.0000(0)	1.9990(0)
N2	24d	0.7175(2)	0.8366(7)	0.5474(0)	1.0000(0)	1.9990(0)
N3	24d	0.7195(2)	0.6683(2)	0.5294(3)	1.0000(0)	1.9990(0)
H1	24d	0.8930(0)	0.8020(0)	0.5310(0)	1.0000(0)	0.8548(0)
H2	24d	0.8920(0)	0.6930(0)	0.5180(0)	1.0000(0)	0.8548(0)
H3	24d	0.6610(0)	0.8350(0)	0.5420(0)	1.0000(0)	0.8548(0)
H4	24d	0.7500(0)	0.8790(0)	0.5460(0)	1.0000(0)	0.8548(0)
H5	24d	0.6690(0)	0.6680(0)	0.5160(0)	1.0000(0)	0.8548(0)
H6	24d	0.7680(0)	0.6230(0)	0.5060(0)	1.0000(0)	0.8548(0)

Table S4. Photoelectric properties of pc-WLEDs and their color gamut in the CIE 1931 color space.

Phosphors		CCT (K)	LE (lm/W)	Color gamut (% NSTC)	Ref.
Green	Red				
β-sialon:Eu^{2+}	$CaAlSiN_3:Eu^{2+}$	8620	38 (20 mA)	82.1	1
YAG:Ce^{3+}		8000	105 (60 mA)	67.9	2
YAG:Ce^{3+}		4950	59 (20 mA)	68.3	1
β-sialon:Eu^{2+}	$K_2SiF_6:Mn^{4+}$	8611	94 (120 mA)	85.9	3
β-sialon:Eu^{2+}	$K_2NbF_7:Mn^{4+}$	11338	94.68 (120 mA)	86.7	4
$CsPbBr_3$ QDs	$Na_2WO_2F_4:Mn^{4+}$	12123	— (120 mA)	107.1	5
β-sialon:Eu^{2+}	$Cs_2SiF_6:Mn^{4+}$	6880	133 (20 mA)	84.7	6
β-sialon:Eu^{2+}	$K_2NaScF_6:Mn^{4+}$	5986	67.65 (20 mA)	127.3	7
$RbLi(Li_3SiO_4)_2:Eu^{2+}$	$K_2SiF_6:Mn^{4+}$	6221	97.28 (20 mA)	107	8
$Sr_2SiO_4:Eu^{2+}$	$CaAlSiN_3:Eu^{2+}$	8330	103 (60 mA)	74.7	2
$Sr_2Ga_2S_4:Eu^{2+}$	$CaAlSiN_3:Eu^{2+}$	8200	105 (60 mA)	86.4	2
$Ba_{0.75}Al_{11}O_{17.25}:Mn^{2+}$	$K_2SiF_6:Mn^{4+}$	6645	— (20 mA)	107.3	9
$MgAl_2O_4:Mn^{2+}$	$K_2SiF_6:Mn^{4+}$	10342	56.32 (20 mA)	116	10
β-sialon:Eu^{2+}	$Cs_2MnF_6:Si^{4+}$	7856	26.00 (20 mA)	122.3	11
β-sialon:Eu^{2+}	$GA_3AlF_6:Mn^{4+}$	6839	37.29 (20 mA)	108.3	This work

References:

(1) Xie, R. J.; Hirosaki, N.; Takeda, T., Wide Color Gamut Backlight for Liquid Crystal Displays Using Three-Band Phosphor-Converted White Light-Emitting Diodes. *Appl Phys Express* **2009,** *2* (2), 022401.

(2) Oh, J. H.; Kang, H.; Ko, M.; Do, Y. R., Analysis of Wide Color Gamut of Green/Red Bilayered Freestanding Phosphor Film-Capped White LEDs for LCD Backlight. *Opt. Express*

2015, *23* (15), A791-804.
(3) Wang, L.; Wang, X. J.; Kohsei, T.; Yoshimura, K. I.; Izumi, M.; Hirosaki, N.; Xie, R. J., Highly Efficient Narrow-Band Green and Red Phosphors Enabling Wider Color-Gamut LED Backlight for More Brilliant Displays. *Opt. Express* **2015,** *23* (22), 28707-28717.
(4) Lin, H.; Hu, T.; Huang, Q. M.; Cheng, Y.; Wang, B.; Xu, J.; Wang, J. M.; Wang, Y. S., Non-Rare-Earth $K_2XF_7:Mn^{4+}$ (X = Ta, Nb): A Highly-Efficient Narrow-Band Red Phosphor Enabling the Application in Wide-Color-Gamut LCD. *Laser Photonics Rev.* **2017,** *11* (6), 1700148.
(5) Hu, T.; Lin, H.; Cheng, Y.; Huang, Q.; Xu, J.; Gao, Y.; Wang, J.; Wang, Y., A Highly-Distorted Octahedron with a C_{2v} Group Symmetry Inducing an Ultra-Intense Zero Phonon Line in Mn^{4+}-Activated Oxyfluoride $Na_2WO_2F_4$. *J. Mater. Chem. C* **2017,** *5* (40), 10524-10532.
(6) Liu, Y.; Zhou, Z.; Huang, L.; Brik, M. G.; Si, S. C.; Lin, L. T.; Xuan, T. T.; Liang, H. B.; Qiu, J. B.; Wang, J., High-Performance and Moisture- Resistant Red-Emitting $Cs_2SiF_6:Mn^{4+}$ for High-Brightness LED Backlighting. *J. Mater. Chem. C* **2019,** *7* (8), 2401-2407.
(7) Ming, H.; Liu, L. L.; He, S. A.; Peng, J. Q.; Du, F.; Fu, J. X.; Yang, F. L.; Ye, X. Y., An Ultra-High Yield of Spherical $K_2NaScF_6:Mn^{4+}$ Red Phosphor and Its Application in Ultra-Wide Color Gamut Liquid Crystal Displays. *J. Mater. Chem. C* **2019,** *7* (24), 7237-7248.
(8) Zhao, M.; Liao, H. X.; Ning, L. X.; Zhang, Q. Y.; Liu, Q. L.; Xia, Z. G., Next-Generation Narrow-Band Green-Emitting $RbLi(Li_3SiO_4)_2$ $:Eu^{2+}$ Phosphor for Backlight Display Application. *Adv. Mater.* **2018,** *30* (38), e1802489.
(9) Hu, J. Q.; Song, E. H.; Zhou, Y. Y.; Zhang, S. L.; Ye, S.; Xia, Z. G.; Zhang, Q. Y., Non-Stoichiometric Defect-Controlled Reduction toward Mixed-Valence Mn-Doped Hexaaluminates and Their Optical Applications. *J. Mater. Chem. C* **2019,** *7* (19), 5716-5723.
(10) Song, E. H.; Zhou, Y. Y.; Wei, Y.; Han, X. X.; Tao, Z. R.; Qiu, R. L.; Xia, Z. G.; Zhang, Q. Y., A Thermally Stable Narrow-Band Green-Emitting Phosphor $MgAl_2O_4:Mn^{2+}$ for Wide Color Gamut Backlight Display Application. *J. Mater. Chem. C* **2019,** *7* (27), 8192-8198.
(11) Zhang, J. F.; Liu, L. L.; He, S. A.; Peng, J. Q.; Du, F.; Yang, F. L.; Ye, X. Y., Cs_2MnF_6 Red Phosphor with Ultrahigh Absorption Efficiency. *Inorg. Chem.* **2019,** *58* (22), 15207-15215.